Journal of Sound and Vibration (2001) **239**(3), 405–422
doi:10.1006/jsvi.2000.3171, available online at http://www.idealibrary.com on IDEAL®

SEISMIC BEHAVIOUR OF BUTTRESS DAMS: NON-LINEAR MODELLING OF A DAMAGED BUTTRESS BASED ON ARX/NARX MODELS

P. PALUMBO

Enel. Hydro (*formerly ISMES*), *Via Pastrengo*, 9 24068 - *Seriate BG*, *Italy*.
E-mail: *palumbo.pasquale@enel.it*

AND

L. PIRODDI

Dipartimento di Elettronica e Informazione, *Politecnico di Milano*, *Piazza Leonardo da Vinci*, 32 20133 – *Milano*, *Italy*. *E-mail*: *piroddi@elet.polimi.it*

(*Received* 29 *October* 1999, *and in final form* 22 *May* 2000)

The paper reports a full model identification study carried out on a scale model of a dam buttress subjected to seismic-like excitations generated by means of a shake table. The use of linear and non-linear models is discussed, since the buttress has an artificial crack and is subjected to high-intensity inputs. In particular, a suitable class of polynomial NARX models is considered, which captures most of the system dynamics.

Several questions related to the NARX identification methodology are addressed in the paper; use of non-linear models greatly increases model accuracy and reliability, but many specific operational problems arise in practice. In particular, the validity of classical model selection approaches is questionable; satisfactory non-linear models are obtained in this case with many fewer parameters than suggested by conventional performance indices. Also, it is difficult to guarantee a satisfactory model performance in simulation and, sometimes, even stability is hard to obtain.

With reference to specific identified models a further analysis step is carried out, which shows the evolution of the dynamic characteristics of the model in the various phases of the earthquake-like excitation. Also, the role of the particular non-linearities included in the model is discussed.

1. INTRODUCTION

A challenging problem in the monitoring of civil structures is the assessment of damage and cracks caused by seismic events. This requires a consistent modelling technique to be available to describe the dynamics of a structure both in low- and high-input excitation situations, so that the evolution of the structure can be checked to see if any characteristics change during major vibrations. Both temporary and permanent system modifications may be experienced; medium intensity signals affect the behaviour of the system only temporarily by exciting its non-linear dynamics for a limited period of time, whereas high-intensity signals produce permanent structure modifications in terms of stiffness decay. Therefore, some type of non-linear modelling must be implemented to account for structural damage (permanent non-linear dynamic modifications) or simply for the effects of

0022-460X/01/030405 + 18 $35.00/0

high-level vibrational input signals. Also a periodic re-identification of the model is necessary to rearrange the model structure and correct its parameters.

A promising line of research in this area is represented by the use of black-box non-linear models of the NARX/NARMAX family [1, 2], which extend the well-known linear ARX/ARMAX class [3, 4]. While many examples of applications of linear techniques to model identification and dynamic analysis applied to civil structures are given in the recent literature (see, e.g. references [5–8]), only few researchers have extended their interest to non-linear modelling techniques (see, e.g., references [9, 10]).

This is motivated mostly by the difficulties in applying non-linear identification methodologies, and by the lack of methods for the analysis of the non-linear models identified. In fact, model selection remains a largely unsolved problem; that is, it is not clear how to select a non-linear class of parametric models to fit a specific set of data. For polynomial NARX/NARMAX models, several criteria have been proposed in the literature for the selection of suitable regression terms (see, e.g., references [11–14]), but this remains as the more critical part of the non-linear identification algorithms, with much room for further research. Empirical indices, such as the final prediction error (FPE), the Akaike information criterion (AIC) and the minimum description length (MDL) [4, 12], have also been applied to the problem of non-linear model selection, but they rarely yield conclusive proof in favour of a specific model structure. Also, since most of the identification algorithms follow a prediction error approach (the one-step ahead prediction error is minimized), there is no guarantee that the identified models will yield an acceptable performance in simulation; that is, when the predicted outputs are fed back in the model instead of the actual system outputs. It is not unusual for an identified non-linear model with a very small prediction error to become unstable in simulation. In conclusion, many effective identification algorithms are available at present for non-linear identification, but much skill is nevertheless required on the part of the user to achieve consistent modelling.

As for the lack of methods for the analysis of the identified non-linear models, this is only partly true for polynomial NARX models, where the parameters can sometimes considered in direct relationship with those of "physical" models. Also, there has been a major breakthrough in recent years concerning the frequency analysis of these types of non-linear models following the works of Billings and Tsang [15, 16]. This has renewed interest on NARX/NARMAX modelling for mechanical and civil applications [9, 10]. In reference [10] the authors have shown some of the results that may be derived by means of such non-linear frequency analysis tools with reference to the same case that is studied here.

In the present work a thorough modelling study is described, which makes use of experimental data gathered at Enel. Hydro (formerly ISMES) laboratories [17, 18]. A laboratory-scale dam buttress has been subjected to earthquake-like inputs on a shake table and the resulting vibrations have been recorded and analyzed. In order to emphasize the need for non-linear models, different amplitude signals have been employed, varying from low to high intensity, and an artificial crack has been artificially opened in the buttress.

The identification study has been conducted both with linear and non-linear models, which have been compared in terms of classical empirical performance indices; the analysis shows that these indices yield conflicting results and may in fact be impractical for non-linear identification purposes. Alternatively, more compact NARX models have been derived which have an acceptable performance and lend themselves to a more specific analysis which can deliver a much deeper understanding of the system dynamic characteristics. In the paper, attention is focused on a subclass of the polynomial NARX models, both for convenience (the model selection phase is simplified) and physical purposes (a direct interpretation of the model parameters is partly possible in terms of physical vibrational models).

2. THE NON-LINEAR MODEL CLASS

The class of polynomial NARX/NARMAX models [1, 2] has many useful and appealing features for non-linear black-box identification:

- they are a discrete-time straightforward counterpart of non-linear differential equations, so that physical parameters can be directly estimated from them;
- they can model purely linear systems as well as a large class of non-linearities;
- they are *linear-in-the-parameters* models, so that they can be identified with simple algorithms of the least-squares family and with relatively little effort;
- a computer implementation of these models and of the related identification algorithms is straightforward.

In the following, a suitable sub-class of polynomial NARX models is defined, with reference to simple 1-degree-of-freedom (1-DOF) systems, described by the following differential model, with quadratic and cubic non-linearities in the elastic force and damping terms:

$$\ddot{y}(t) = k_{11}\dot{y}(t) + k_{12}\dot{y}(t)^2 + k_{13}\dot{y}(t)^3 + k_{01}y(t) + k_{02}y(t)^2 + k_{03}y(t)^3 + k_2 u(t).$$

The corresponding NARX structure is derived from the last expression by a standard approximate Euler discretization:

$$\begin{aligned} y(k) = {} & c_{1,0}(1)y(k-1) + c_{1,0}(2)y(k-2) + c_{2,0}(1,1)y(k-1)^2 + c_{2,0}(1,2)y(k-1)y(k-2) \\ & + c_{2,0}(2,2)y(k-2)^2 + c_{3,0}(1,1,1)y(k-1)^3 + c_{3,0}(1,1,2)y(k-1)^2 y(k-2) \\ & + c_{3,0}(1,2,2)y(k-1)y(k-2)^2 + c_{3,0}(2,2,2)y(k-2)^3 + c_{0,1}(1)u(k-1). \end{aligned}$$

The parameter notation, borrowed from reference [19], must be interpreted as follows; the first subscript index denotes the number of $y(\cdot)$ factors in the corresponding regression term, whereas the second index refers to the number of $u(\cdot)$ factors; the numbers in parentheses are the time delays of the various factors in the regression term [$y(\cdot)$ factors first].

Extending this approach, the following "extended" model structure, which can capture up to four vibrational modes in the linear part, is obtained:

$$\begin{aligned} y(k) = {} & c_{0,0} + \sum_{1}^{8} {}_{k_1} c_{1,0}(k_1)y(k-k_1) + \sum_{1}^{4} {}_{k_1} \sum_{k_1}^{4} {}_{k_2} c_{2,0}(k_1,k_2)y(k-k_1)y(k-k_2) \\ & + \sum_{1}^{4} {}_{k_1} \sum_{k_1}^{4} {}_{k_2} \sum_{k_2}^{4} {}_{k_3} c_{3,0}(k_1,k_2,k_3)y(k-k_1)y(k-k_2)y(k-k_3) + \sum_{1}^{4} {}_{k_1} c_{0,1}(k_1)u(k-k_1). \end{aligned} \tag{1}$$

Model (1), though heavily restricted in the type of non-linearity, is nevertheless capable of describing efficiently most of the dynamic properties of the structure analyzed in the following. As already pointed out, restricting the number of regressors in the identification process is a key feature to successful modelling, in that it simplifies the model selection phase. However, the methods shown below can be easily extended to more general classes of NARX models.

The identification of linearly parameterized polynomial models of type (1) can be easily performed with standard least squares. However, orthogonalization procedures are usually employed in the selection of the appropriate regression terms in order to prevent numerical problems in the identification procedure [11].

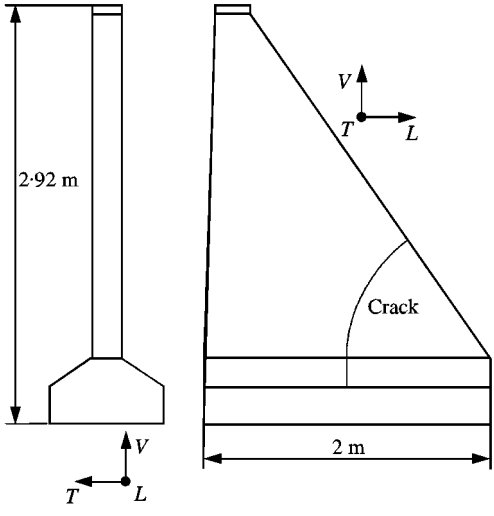

Figure 1. The dam buttress scale model.

3. THE DAM BUTTRESS DATA

All the results produced in the paper pertain to experimental data gathered at ISMES laboratories [17, 18] as follows: a scale model of a dam buttress (Figure 1) has been subjected to seismic-like signals at different excitation levels on a shake table and the resulting vibrations have been measured in different places of the buttress.

The buttress has been constructed with homogeneous and isotropic materials which have a linear elastic behaviour in the applied excitation range. An artificial closed crack has been produced in the buttress, so that non-linear behaviour is to be expected, especially with high-amplitude input signals. In loose terms, structural movements that tend to open the crack are wider than movements in the opposite direction, resulting in asymmetrical oscillations, i.e., in a non-linear type of motion.

The experimental set-up has been developed in order to study one of the typical non-linearities that may be experienced in real-dam buttresses. However, it must be kept in mind that the actual modal parameters of this scale model have no relationship with those usually measured in structures of this type.

The shake table is capable of generating six simultaneous and independent motions (three translational and three rotational with respect to three orthogonal axes). It is driven by four horizontal and four vertical electro-hydraulic actuators, which can exert a force of 500 and 600 kN respectively. Altogether, 75 measurement points have been placed on the buttress in the three orthogonal directions (marked L, T and V in Figure 1) in various positions. Acceleration measurements are taken by means of piezoeletric accelerometers.

Performing model identification at different excitation levels has pointed out the dependency of structural parameters of the system on the input amplitude, thus revealing its non-linear nature. Three experimental recordings, which correspond to low, medium and high input amplitude, respectively, are considered in the sequel [18]. The time-domain diagrams of the recorded data are reported in Figures 2–4. Both input and output signals are acceleration measurements (m/s^2) in the longitudinal direction (marked L in Figure 1); the inputs are measured at the base of the buttress, while the outputs are taken at the top. Data are sampled every 2×10^{-3} s for a total period of 10 s (5000 data points).

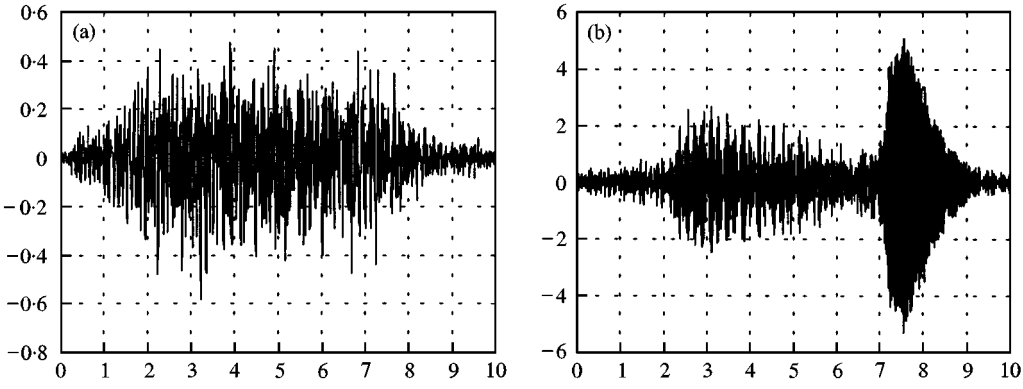

Figure 2. (a) Input signal (low-force data set). (b) Output signal (low-force data set).

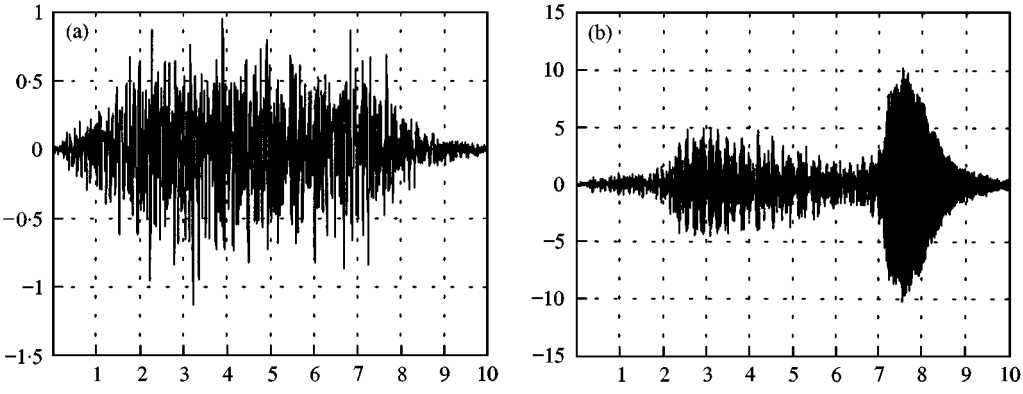

Figure 3. (a) Input signal (medium-force data set). (b) Output signal (medium-force data set).

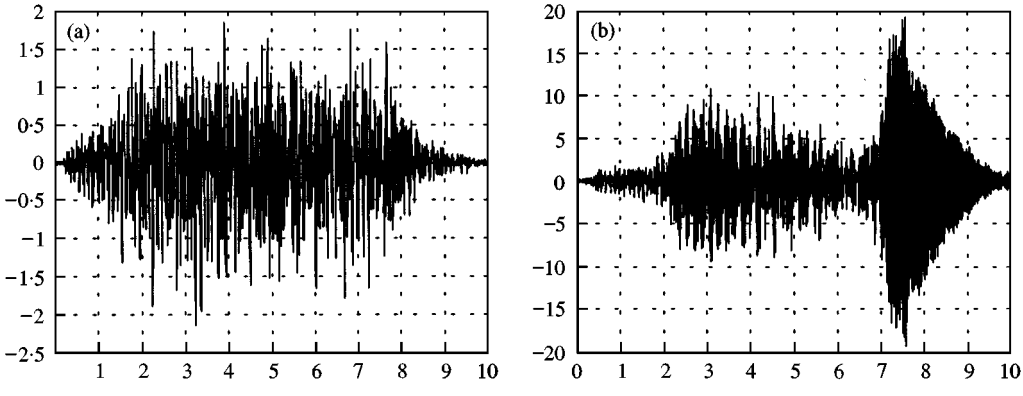

Figure 4. (a) Input signal (high-force data set). (b) Output signal (high-force data set).

The spectral diagrams are shown in Figures 5 and 6. These have been computed on the raw data with standard FFT-based routines, with a Hamming window of lag size 30. No further filtering has been applied to the signals, so as not to attenuate significant high-frequency dynamics if any. The spectra display a resonance peak between 40 and

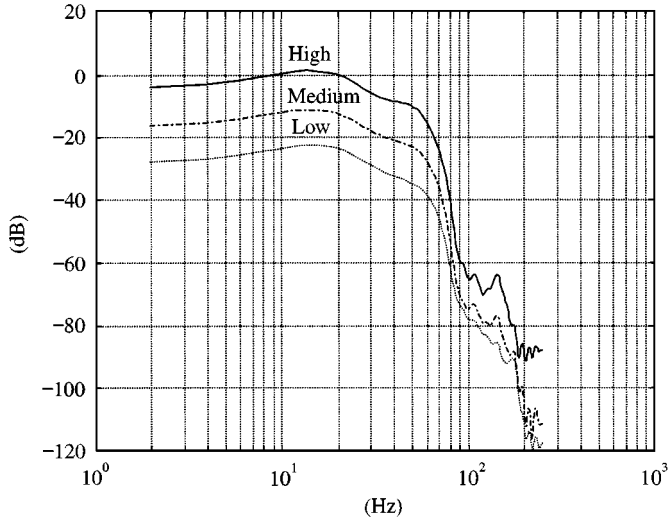

Figure 5. Spectral diagram: input signals.

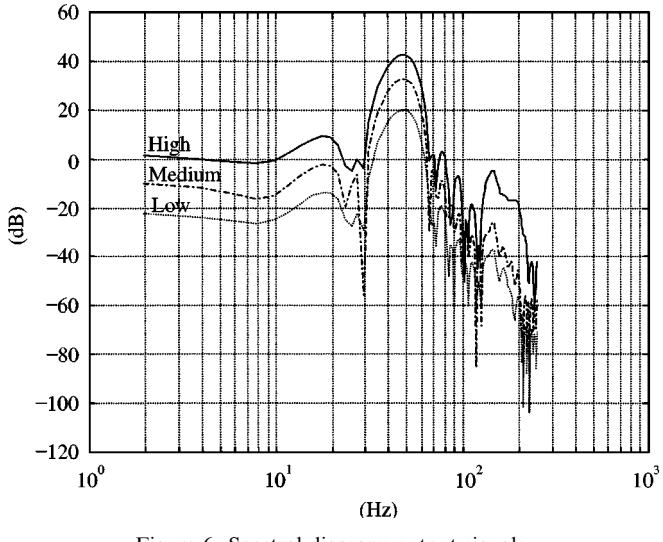

Figure 6. Spectral diagram: output signals.

50 Hz and other lower but significant peaks, clearly distinguishable from high-frequency ripples. These additional peaks are most probably not the effect of high-frequency noise in the measurements but of an inherent non-linearity of the system; in particular, the peaks at the double and triple of the resonance frequency (*harmonics*) call for a quadratic and/or cubic NARX model. This is particularly true for the data corresponding to a high-amplitude input signal. This intuition is confirmed by the time diagrams (examine the time interval between 2 and 6 s), where an asymmetry is apparent.

Note also that while the input spectrum drops abruptly after 70 Hz, the output displays a much larger band; this phenomenon is probably due to a combination of factors, such as the presence of high-frequency noise in the measurements, and a non-linear behaviour of the system (a noise-free linear system cannot generate harmonic components at frequencies not contained in the input spectrum).

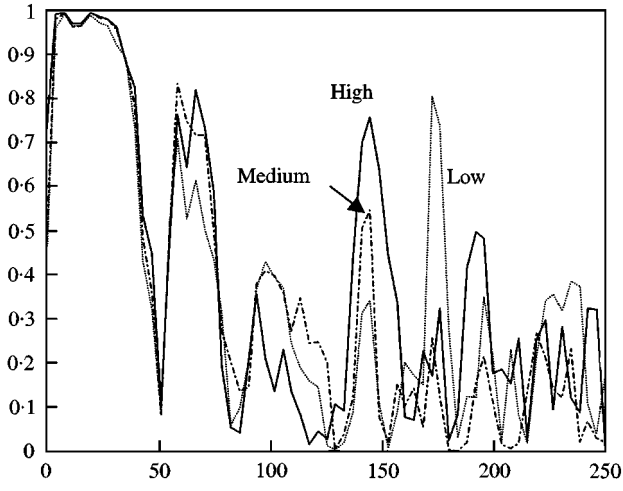

Figure 7. Coherence functions.

4. LINEAR OR NON-LINEAR MODELLING?

A typical means for establishing the need of a non-linear model is the coherence function, which indicates the frequency bands where the input–output relationship can be safely interpreted as being linear. Figure 7 shows the coherence functions of the three data sets. In all cases, a linear model is shown to be sufficient in order to capture the low-band behaviour. However, the coherence function is very low in the proximity of the resonance peak. Also, as has already been pointed out, there are still some relevant dynamics to be modelled in the medium frequency band (50–150 Hz). From the coherence diagrams it appears that these features require non-linear modelling.

A different type of analysis has been performed next. A linear ARX(8, 8) model has been estimated for every data set and the frequency response diagram associated with the transfer function of the model has been analyzed. The linear model is chosen to be redundant on purpose so that it has a sufficient number of degrees of freedom to capture also the dynamics that relate to the non-linear behaviour of the system. All three diagrams (Figure 8) show a resonance peak at about 48 Hz with an amplitude of 35–40 dB. Two other peaks of

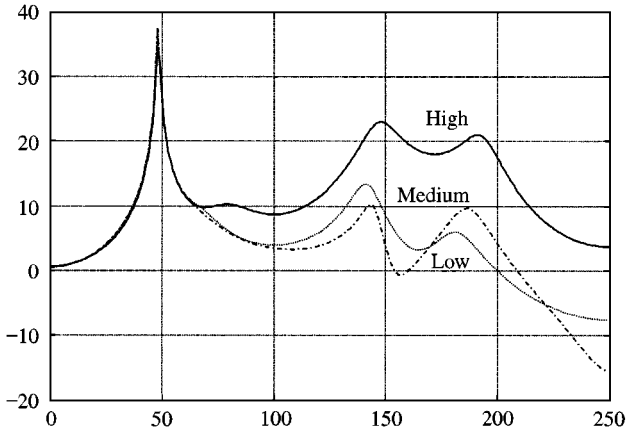

Figure 8. Redundant linear model frequency response diagram.

lower amplitude occur at ~ 144 Hz (48×3 Hz) and ~ 192 Hz (48×4 Hz) respectively. Since these peaks are located at a frequency which is almost equal to three and four times the fundamental frequency, respectively, it can be argued that an appropriate model should contain non-linearities of the cubic quadratic type. In particular, the secondary peaks of the ARX model estimated on the high force data set have an amplitude almost equivalent to that of the peak at the fundamental frequency.

5. MODEL IDENTIFICATION

Extensive model identification sessions have been performed in order to select suitable model structures and parameterizations for all the data sequences. Both linear ARX and non-linear NARX models have been analyzed. The following families of models have been considered:

- *linear models*: ARX(n_a, n_b),
- *non-linear models*: NARX(n_a, n_b, 1) (linear ARX(n_a, n_b) models augmented with a single cubic term $y(k-1)^3$),
- *non-linear models*: NARX(n_a, n_b, 2) (linear ARX(n_a, n_b) models augmented with the regression terms $y(k-1)^2$ and $y(k-1)^3$),

where n_a represents the number of autoregressive terms of the model and n_b is the number of exogenous terms ($n_a = 4$, 6, 8, 10, 12, 14, 16, 18, 20, 22, 24 and $n_b = 4$).

Only these simple non-linearities have been included in the model structure, motivated by the conclusions drawn at the end of the previous paragraph.

The most critical aspect in the identification methodology is represented by the selection of the appropriate model structure; the model should simulate the underlying system with sufficient accuracy, at the same time filtering the spurious or noisy information contained in the input/output data. In other words, the model should be both *precise* (minimal prediction and simulation error) and *robust* (accuracy also on data not employed in the estimation phase). Note that the precision, that is, the ability of a model to fit the data, increases with its complexity (i.e., the number of parameters), whereas beyond a certain limit robustness decreases, since the model overfits the data employed in estimation and is less generalizable to other data.

There exist several different tools for the evaluation of the quality of an estimated model [3, 4]:

(1) computation of objective indices as the prediction or simulation error variance;
(2) computation of empirical indices (FPE, AIC, MDL), that compromise between accuracy and complexity of the estimated model;
(3) correlation analysis (auto-correlation of the prediction error and cross-correlation between prediction error and input);
(4) cross-validation (evaluation of the quality of the model on data different from those employed in estimation).

The analysis performed in the paper has shown that tools of the first three types may yield results which are not conclusive or which are difficult to interpret for the selection of the model structure.

The identified models have been compared in terms of both objective indices, such as the prediction error variance and the simulation error variance, and empirical indices, such as the FPE, the AIC and the MDL [4, 12]. These indices, which have been conceived with

reference to stationary stochastic processes, are employed in the following to evaluate their usefulness in a wider context. They are defined as follows:

$$\mathrm{FPE} = \frac{N+n}{N-n} J_n(\hat{\vartheta}_n),$$

$$\mathrm{AIC} = \log(J_n(\hat{\vartheta}_n)) + 2\frac{n}{N},$$

$$\mathrm{MDL} = \log(J_n(\hat{\vartheta}_n)) + \log(N)\frac{n}{N},$$

where $J_n(\hat{\vartheta}_n)$ is the prediction error variance of the estimated model (which depends on the estimated model parameterization $\hat{\vartheta}_n$), n is the total number of parameters and N is the number of data employed in the estimation. The best model according to each of these indices is such that incrementing further the number of parameters does not diminish significantly the index. Usually, the three methods give correlated answers: for high N the FPE and the AIC select almost equal models, while the MDL generally selects a model with fewer parameters than the other two methods.

In Tables 1–3, model performances are compared in terms of these five indices for each of the three data sets. Shading indicates the minimum value obtained for the error variances and the best model structure selected according to the empirical indices.

Finally, all identified models have been subjected to classical correlation tests to certify that they have the appropriate structure with respect to the true system. These tests are based on the observation that the residual should ideally be a zero mean white noise and be independent of all inputs: the validity of these hypotheses is statistically checked by the examination of the residual autocorrelation function and the input-residual cross-correlation function respectively. If these functions are not significantly different from zero, i.e., they are inside suitable confidence bands, the residual is assumed to be of the desired type.

5.1. MODEL IDENTIFICATION OF THE LOW-FORCE DATA SET

As can be seen from Table 1, 16 autoregressive terms are needed in this case. More linear terms result in a slight increase of FPE, whereas AIC and MDL display an insignificant improvement. The use of one of more non-linear terms does not alter this performance. However, it must be noted that, comparing models with the same number of autoregressive parameters, the NARX(n_a, n_b, 1) models display a better simulation error. If the latter is taken as the reference index, one should select models with 16 autoregressive parameters.

For models with $n_a \geqslant 14$ the linear part of the model is redundant; by inspection of the transfer function many couples of poles and zeros may be seen to be almost in the same positions (quasi-cancellations). The prediction error autocorrelation and the cross-correlation between the input and the prediction error are minimal for models with $n_a \geqslant 16$.

5.2. MODEL IDENTIFICATION OF THE MEDIUM-FORCE DATA SET

Again, the FPE, AIC and MDL indices suggest that 16 autoregressive terms should be included in the model, whereas the use of additional non-linear terms is ineffective (see

TABLE 1

Comparison of the models estimated on the low-force data set

	Pred. err. variance	Sim. err. variance	FPE	AIC	MDL
ARX(4, 4)	0·005667	0·2013	0·0057	−5·1698	−5·1594
ARX(6, 4)	0·005024	0·1869	0·0050	−5·2895	−5·2765
ARX(8, 4)	0·004085	0·2049	0·0041	−5·4956	−5·4800
ARX(10, 4)	0·003644	0·1700	0·0037	−5·6089	−5·5907
ARX(12, 4)	0·003382	0·1663	0·0034	−5·6830	−5·6622
ARX(14, 4)	0·003223	0·1845	0·0032	−5·7304	−5·7069
ARX(16, 4)	0·002788	0·1621	0·0028	−5·8744	−5·8483
ARX(18, 4)	0·002728	0·1729	0·0028	−5·8952	−5·8666
ARX(20, 4)	0·002666	0·1625	0·0027	−5·9175	−5·8863
ARX(22, 4)	0·002648	0·1631	0·0027	−5·9236	−5·8897
ARX(24, 4)	0·002642	0·1645	0·0027	−5·9249	−5·8884
NARX(4, 4, 1)	0·005660	0·1998	0·0057	−5·1707	−5·1590
NARX(6, 4, 1)	0·005020	0·1830	0·0050	−5·2899	−5·2756
NARX(8, 4, 1)	0·004070	0·1884	0·0041	−5·4989	−5·4819
NARX(10, 4, 1)	0·003641	0·1594	0·0037	−5·6096	−5·5901
NARX(12, 4, 1)	0·003377	0·1552	0·0034	−5·6838	−5·6617
NARX(14, 4, 1)	0·003216	0·1730	0·0032	−5·7320	−5·7073
NARX(16, 4, 1)	0·002783	0·1513	0·0028	−5·8759	−5·8485
NARX(18, 4, 1)	0·002723	0·1625	0·0027	−5·8967	−5·8667
NARX(20, 4, 1)	0·002662	0·1544	0·0027	−5·9187	−5·8861
NARX(22, 4, 1)	0·002642	0·1522	0·0027	−5·9254	−5·8902
NARX(24, 4, 1)	0·002636	0·1531	0·0027	−5·9268	−5·8890
NARX(4, 4, 2)	0·005652	0·1995	0·0057	−5·1718	−5·1587
NARX(6, 4, 2)	0·005017	0·1830	0·0050	−5·2902	−5·2746
NARX(8, 4, 2)	0·004062	0·1883	0·0041	−5·5005	−5·4823
NARX(10, 4, 2)	0·003637	0·1592	0·0037	−5·6103	−5·5894
NARX(12, 4, 2)	0·003372	0·1548	0·0034	−5·6850	−5·6615
NARX(14, 4, 2)	0·003214	0·1726	0·0032	−5·7323	−5·7063
NARX(16, 4, 2)	0·002782	0·1512	0·0028	−5·8757	−5·8471
NARX(18, 4, 2)	0·002722	0·1625	0·0027	−5·8968	−5·8656
NARX(20, 4, 2)	0·002661	0·1544	0·0027	−5·9186	−5·8847
NARX(22, 4, 2)	0·002642	0·1521	0·0027	−5·9252	−5·8887
NARX(24, 4, 2)	0·002636	0·1530	0·0027	−5·9266	−5·8875

Table 2). The simulation error variance confirms that purely linear models are enough in this case. Also, it indicates that an appropriate number of autoregressive parameters should be 10, 12 or 16. It must be noted, however, that none of the identified models respects the 95% confidence bands of the residual autocorrelation and the input-residual cross-correlation. More than 16 linear autoregressive terms are clearly redundant.

5.3. MODEL IDENTIFICATION OF THE HIGH-FORCE DATA SET

The FPE, AIC and MDL indices unanimously show that the high-force data set is best estimated with 14 autoregressive terms and, as expected, the non-linear terms significantly increase the estimation performance (see Table 3). Interestingly enough, the best performance in terms of the simulation error is obtained in correspondence with very

TABLE 2

Comparison of the models estimated on the medium-force data set

	Pred. err. variance	Sim. err. variance	FPE	AIC	MDL
ARX(4, 4)	0·015467	0·5103	0·0155	−4·1659	−4·1555
ARX(6, 4)	0·015174	0·4926	0·0152	−4·1842	−4·1711
ARX(8, 4)	0·012279	0·5456	0·0123	−4·3951	−4·3795
ARX(10, 4)	0·011232	0·4582	0·0113	−4·4834	−4·4651
ARX(12, 4)	0·011035	0·4476	0·0111	−4·5003	−4·4794
ARX(14, 4)	0·010242	0·4878	0·0103	−4·5741	−4·5506
ARX(16, 4)	0·009696	0·4758	0·0098	−4·6280	−4·6020
ARX(18, 4)	0·009643	0·4857	0·0097	−4·6327	−4·6040
ARX(20, 4)	0·009623	0·4883	0·0097	−4·6340	−4·6027
ARX(22, 4)	0·009538	0·4694	0·0096	−4·6420	−4·6081
ARX(24, 4)	0·009485	0·4858	0·0096	−4·6469	−4·6104
NARX(4, 4, 1)	0·015275	0·6684	0·0153	−4·1779	−4·1662
NARX(6, 4, 1)	0·014954	0·6956	0·0150	−4·1984	−4·1840
NARX(8, 4, 1)	0·012237	0·6155	0·0123	−4·3981	−4·3812
NARX(10, 4, 1)	0·011149	0·6403	0·0112	−4·4904	−4·4709
NARX(12, 4, 1)	0·010970	0·6003	0·0110	−4·5058	−4·4836
NARX(14, 4, 1)	0·010218	0·5549	0·0103	−4·5760	−4·5512
NARX(16, 4, 1)	0·009659	0·5911	0·0097	−4·6315	−4·6041
NARX(18, 4, 1)	0·009611	0·5901	0·0097	−4·6357	−4·6057
NARX(20, 4, 1)	0·009591	0·5930	0·0097	−4·6369	−4·6044
NARX(22, 4, 1)	0·009516	0·5522	0·0096	−4·6440	−4·6088
NARX(24, 4, 1)	0·009469	0·5495	0·0096	−4·6481	−4·6103
NARX(4, 4, 2)	0·015275	0·6684	0·0153	−4·1775	−4·1645
NARX(6, 4, 2)	0·014954	0·6956	0·0150	−4·1980	−4·1824
NARX(8, 4, 2)	0·012237	0·6155	0·0123	−4·3977	−4·3795
NARX(10, 4, 2)	0·011148	0·6402	0·0112	−4·4901	−4·4692
NARX(12, 4, 2)	0·010970	0·6003	0·0110	−4·5054	−4·4819
NARX(14, 4, 2)	0·010218	0·5550	0·0103	−4·5756	−4·5496
NARX(16, 4, 2)	0·009657	0·5914	0·0097	−4·6313	−4·6026
NARX(18, 4, 2)	0·009609	0·5904	0·0097	−4·6354	−4·6041
NARX(20, 4, 2)	0·009590	0·5933	0·0097	−4·6367	−4·6028
NARX(22, 4, 2)	0·009514	0·5523	0·0096	−4·6438	−4·6073
NARX(24, 4, 2)	0·009466	0·5497	0·0096	−4·6480	−4·6089

parsimonious models: NARX(4, 4, 1), NARX(4, 4, 2), NARX(6, 4, 1), NARX(6, 4, 2). All identified models should be rejected on the basis of the correlation tests. For the models with $n_a \geqslant 20$, the linear part is redundant.

5.4. SOME COMMENTS AND FURTHER DEVELOPMENTS

The identification compaign has shown several interesting facts:

(1) The low- and medium-force data sets are effectively estimated by linear models whereas the high-amplitude input case requires some non-linear modelling, indicating that the input intensity is enough to excite the non-linear dynamics of the system.
(2) If the simulation error is considered, better results are obtained in both the low- and high-force cases if NARX(n_a, n_b, 1), models are employed. Additional non-linear terms are ineffective.

TABLE 3

Comparison of the models estimated on the high-force data set

	Pred. err. variance	Sim. err. variance	FPE	AIC	MDL
ARX(4, 4)	0·278522	4·6207	0·2794	−1·2751	−1·2646
ARX(6, 4)	0·236060	4·4829	0·2370	−1·4397	−1·4266
ARX(8, 4)	0·190917	4·7018	0·1918	−1·6511	−1·6355
ARX(10, 4)	0·184794	4·5701	0·1858	−1·6829	−1·6647
ARX(12, 4)	0·180552	4·5721	0·1817	−1·7053	−1·6845
ARX(14, 4)	0·175394	4·5932	0·1767	−1·7335	−1·7101
ARX(16, 4)	0·174656	4·5961	0·1761	−1·7369	−1·7109
ARX(18, 4)	0·174012	4·6489	0·1756	−1·7398	−1·7112
ARX(20, 4)	0·171164	4·7730	0·1728	−1·7555	−1·7243
ARX(22, 4)	0·170478	4·8018	0·1723	−1·7587	−1·7249
ARX(24, 4)	0·169331	4·7818	0·1712	−1·7647	−1·7282
NARX(4, 4, 1)	0·276450	3·7756	0·2774	−1·2821	−1·2704
NARX(6, 4, 1)	0·234322	3·8792	0·2354	−1·4467	−1·4323
NARX(8, 4, 1)	0·189218	4·2417	0·1902	−1·6597	−1·6427
NARX(10, 4, 1)	0·182947	4·0606	0·1840	−1·6926	−1·6730
NARX(12, 4, 1)	0·178784	4·0514	0·1800	−1·7148	−1·6926
NARX(14, 4, 1)	0·173921	4·0266	0·1752	−1·7416	−1·7168
NARX(16, 4, 1)	0·173063	4·0170	0·1745	−1·7457	−1·7183
NARX(18, 4, 1)	0·172312	4·0355	0·1739	−1·7493	−1·7193
NARX(20, 4, 1)	0·169633	4·0993	0·1713	−1·7641	−1·7315
NARX(22, 4, 1)	0·169016	4·1269	0·1709	−1·7670	−1·7318
NARX(24, 4, 1)	0·167785	4·1023	0·1697	−1·7735	−1·7357
NARX(4, 4, 2)	0·275148	3·7786	0·2763	−1·2864	−1·2734
NARX(6, 4, 2)	0·233804	3·8820	0·2349	−1·4485	−1·4328
NARX(8, 4, 2)	0·188739	4·2399	0·1898	−1·6618	−1·6435
NARX(10, 4, 2)	0·182430	4·0580	0·1836	−1·6950	−1·6741
NARX(12, 4, 2)	0·178068	4·0495	0·1794	−1·7184	−1·6949
NARX(14, 4, 2)	0·173286	4·0250	0·1747	−1·7448	−1·7187
NARX(16, 4, 2)	0·172455	4·0153	0·1740	−1·7488	−1·7201
NARX(18, 4, 2)	0·171621	4·0342	0·1733	−1·7529	−1·7216
NARX(20, 4, 2)	0·168845	4·1001	0·1706	−1·7684	−1·7345
NARX(22, 4, 2)	0·168294	4·1256	0·1702	−1·7708	−1·7343
NARX(24, 4, 2)	0·167060	4·0973	0·1691	−1·7774	−1·7383

(3) Apparently, all the empirical criteria (FPE, AIC and MDL) give identical results. This is to be expected for FPE and AIC, but is not usually experimented with MDL, which tends to select more parsimonious models than the first two indices. In the specific case, this must be ascribed to the extremely large number of data with respect to the number of parameters considered: if $N \gg n$, the prediction error variance is weighted much more than the model complexity, so that there is little difference in selecting the model structure on the basis of the prediction error variance or of one of the empirical criteria. On the other hand, substantially different model structures are suggested by the simulation error variance, which evaluates the model on a totally different basis. This questions whether simulation- or prediction-based indices should be considered to be more reliable. This could largely depend on issues related to the final purpose of the models; if the model are estimated for interpretation purposes, prediction accuracy could be insufficient.

(4) In most cases many autoregressive terms are necessary, but the high-force data set shows that fewer (but appropriate) non-linear terms could be equivalent; an increase in the linear terms of the model cannot compensate for an inherent non-linearity of the system.

This last point can be better understood if the significance of the parameter estimates is evaluated with the standard analysis methods for least-squares estimates [4]. The convariance matrix of the estimated parameter vector can be computed using the formula

$$\mathrm{cov}(\hat{\vartheta}) = \hat{\lambda}^2 \left[\sum_{1}^{N} \varphi(k)\varphi(k)' \right]^{-1},$$

where $\hat{\vartheta}$ is the estimated parameter vector, $\varphi(k)$ is the regressor vector and $\hat{\lambda}^2$ is the estimated variance of the prediction residual. The estimated parameters are considered significantly different from 0 if their absolute value is much greater than three times, $\hat{\sigma}$, where the latter denotes the standard deviation of the parameters (the $\hat{\sigma}$ values can be computed by taking the square root of the main diagonal elements of the covariance matrix). Now, with reference to the high-force data set, if for example model ARX(24, 4) is considered, nearly half of the parameters fail this statistical test, so that the model can be considered highly redundant (statistically not significant parameters are shaded in Table 4).

On the other hand, if the same test is performed on the NARX(4, 4, 1) model, all the parameters are considered significant (see Table 5).

Finally, it should be noted that the procedure for the selection of the appropriate terms in the model is based on the predication error variance, and it is not infrequent that the indentified model turns out to be unstable if tested in simulation mode. While this was not the case for the model classes investigated in sections 5.1–5.3, it is true for general polynomial NARX models and also for the reference model (1) used here. Much trial and error is required on the part of the user to obtain a model which is stable at least on the same data set used for identification. At present, this constitutes a major drawback in NARX model identification.

TABLE 4

Significance of the parameters estimated for the ARX(24, 4) model on the high-force data set

Parameter	Value	$3\hat{\sigma}$	Parameter	Value	$3\hat{\sigma}$
$c_{1,0}(1)$	0·6774	0·0425	$c_{1,0}(15)$	−0·0388	0·07494
$c_{1,0}(2)$	−0·6739	0·0500	$c_{1,0}(16)$	0·0275	0·0792
$c_{1,0}(3)$	0·4988	0·0576	$c_{1,0}(17)$	−0·0680	0·0770
$c_{1,0}(4)$	−1·0061	0·0609	$c_{1,0}(18)$	0·0963	0·0748
$c_{1,0}(5)$	0·2980	0·0743	$c_{1,0}(19)$	−0·0813	0·0739
$c_{1,0}(6)$	−0·4710	0·0743	$c_{1,0}(20)$	0·0019	0·0704
$c_{1,0}(7)$	0·3122	0·0769	$c_{1,0}(21)$	−0·0005	0·0592
$c_{1,0}(8)$	−0·4469	0·0780	$c_{1,0}(22)$	−0·0647	0·0549
$c_{1,0}(9)$	−0·0349	0·0800	$c_{1,0}(23)$	0·0949	0·0491
$c_{1,0}(10)$	0·1061	0·0794	$c_{1,0}(24)$	−0·0478	0·0299
$c_{1,0}(11)$	0·0835	0·0794	$c_{0,1}(1)$	0·7784	0·3507
$c_{1,0}(12)$	0·0332	0·0786	$c_{0,1}(2)$	−1·4544	0·9244
$c_{1,0}(13)$	−0·1865	0·0791	$c_{0,1}(3)$	2·8631	1·0118
$c_{1,0}(14)$	0·1259	0·0797	$c_{0,1}(4)$	−0·3810	0·4996

TABLE 5

Significance of the parameters estimated for the $NARX(4,4,1)$ model on the high-force data set

Parameter	Value	$3\hat{\sigma}$
$c_{1,0}(1)$	0·9074	0·0285
$c_{1,0}(2)$	−0·5279	0·0419
$c_{1,0}(3)$	0·4576	0·0422
$c_{1,0}(4)$	−0·7067	0·0278
$c_{3,0}(1)$	$-1{\cdot}2745 \times 10^{-4}$	$0{\cdot}6254 \times 10^{-4}$
$c_{0,1}(1)$	1·4789	0·4015
$c_{0,1}(2)$	−3·3362	1·0046
$c_{0,1}(3)$	5·0140	1·0042
$c_{0,1}(4)$	−2·2512	0·4017

6. SOME FURTHER ANALYSIS

A deeper understanding of the dynamic behaviour of the system can be obtained by repeating the model identification as the input excitation progresses. For reasons of convenience this analysis has been limited to the high-force data set and only the following parsimonious NARX model structure has been considered:

$$y(k) = c_{1,0}(1)y(k-1) + c_{1,0}(2)y(k-2) + c_{1,0}(3)y(k-3) + c_{1,0}(4)y(k-4)$$
$$+ c_{3,0}(1,1,1)y(k-1)^3 + c_{0,1}(1)u(k-1), \tag{2}$$

with only six parameters and a time window restricted to the last four time steps.

To account for the high non-stationarity of the signals, the data set has been divided in partially overlapping 2 s blocks, which roughly discriminate the various phases of the vibrational motion.

A harmonic analysis of these models based on the use of generalized frequency response functions has been reported in reference [10]; this reveals, as expected, a "softening spring" behaviour of the structure. In fact, the resonance peak of the identified model decreases as the input amplitude increases. This can be interpreted as an effect of the structural damage in the buttress and shows how the method can be used for the monitoring of structures.

Analogous conclusions can be drawn by examining the model variation during the period of maximum input excitation. In fact, if model (2) is re-estimated for the subsequent data blocks in the 6–7, 7–8, 8–9 and 9–10 s time intervals, the poles of the linear part of the model move as shown in Table 6 (see also Figure 9).

Notice that one of the couples of complex conjugated poles remains almost fixed on the unit circle, whereas the other couple varies considerably in phase and much less in the modulus. The former accounts for the peak at the fundamental frequency; in the 7–8 s case (maximum signal intensity) this couple displays the minimum phase, which can be otherwise interpreted as being associated with the lowest fundamental frequency.

Considering the magnitude of the poles, one would conclude that the linear part of the model is unstable in the 7–8 s time window. In any case all the estimated models have some poles very near the unit circle, due to the high oscillating nature of the signals involved.

TABLE 6

Poles of the linear part of model (2) *estimated at different time intervals*

6–7 s	7–8 s	8–9 s	9–10 s
0·8088 ± 0·5719i	0·8342 ± 0·5551i	0·8202 ± 0·5596i	0·8181 ± 0·5634i
−0·3529 ± 0·7583i	−0·4012 ± 0·7312i	−0·2631 ± 0·8048i	−0·1398 ± 0·8433i

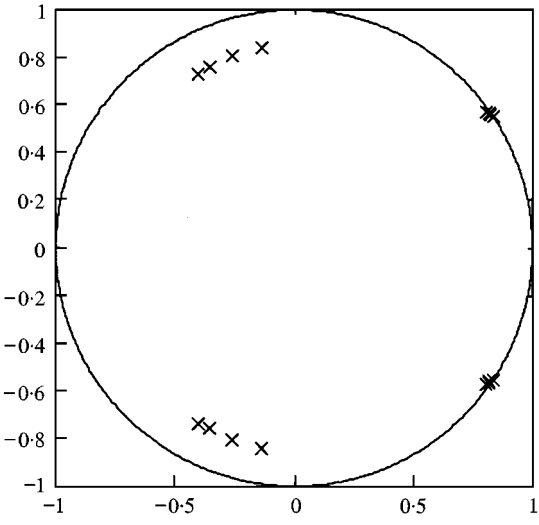

Figure 9. Location of the poles of the linear part of model (2) estimated at different time intervals.

TABLE 7

Natural frequencies and damping factors of the dominant poles at different time intervals

Time window (s)	First pole	Frequency	Damping
6–7	0·8088 + 0·5719i	48·98	0·0154
7–8	0·8342 + 0·555i	46·72	−0·0034
8–9	0·8202 + 0·5596i	47·64	0·0119
9–10	0·8181 + 0·5634i	47·99	0·0111

The corresponding natural frequencies (f_j) and damping factors (ξ_j) can be computed as in reference [20]:

$$\xi_j = \frac{\ln(1/r_j)}{\sqrt{\phi_j^2 + \ln^2(1/r_j)}}, \quad f_j = \frac{\ln(1/r_j)}{2\pi\xi_j T},$$

where r_j and ϕ_j are the magnitude and phase of the jth couple of complex poles, respectively, and T is the sampling time. With reference to the dominant poles the values of natural frequencies and damping factors reported in Table 7 are obtained.

The first order frequency response function (Figure 10) displays a single significant resonance peak corresponding to the frequency values reported in Table 7;

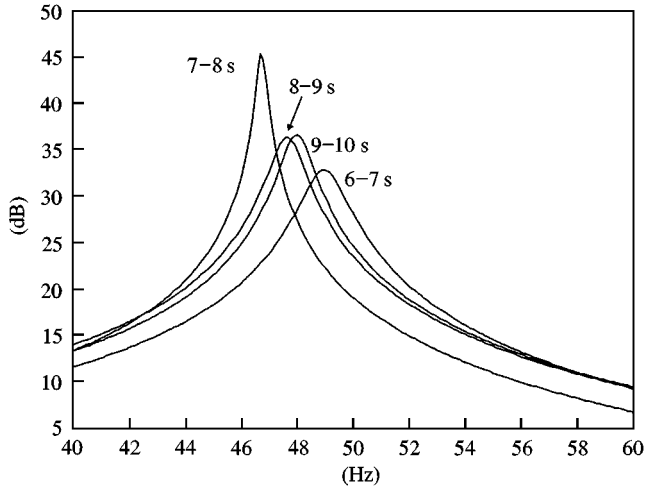

Figure 10. Frequency response function associated with the linear part of the models estimated at different time windows.

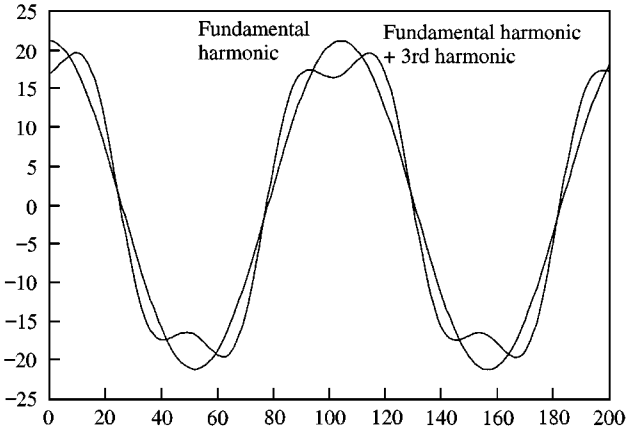

Figure 11. Effect of the cubic non-linear term in the systems's response.

it can be observed that the frequency of the peak decreases as the output signal amplitude excursion gets higher (7–8 s), and that afterwards it gradually returns at higher values.

The characteristic role of the cubic non-linearity included in the model is clearly seen in the time domain, if the model is simulated with single-frequency inputs which excite the higher order harmonics of the system's response. For example, the steady state response to the input signal $u(k) = 30\cos(2\pi 30k)$ looks like the one depicted in Figure 11; if compared with the linearlized model response, a significant contribution of the harmonic component at 90 Hz is evident.

Suppose now the system is subjected to a bi-tonal input $u(k) = 10\cos(2\pi 30k) + 10\cos(2\pi 40k)$. In this case, several frequencies are excited in the response apart from f_1 and f_2, which are already present in the input; the third harmonics ($3f_1$, $3f_2$) appear, as well as the terms corresponding to sum ($2f_1 + f_2$, $f_1 + 2f_2$) and difference frequencies ($|f_1 - f_2|$, $|2f_1 - f_2|$). The magnitudes of the various frequency components of the output signal are reported in Table 8.

TABLE 8

Intermodulation effect

Frequency	Hz	Magnitude	
		Non-linear model	Linear model
$\|f_1 - f_2\|$	10	7·4904	0
$\|2f_1 - f_2\|$	20	112·101	0
f_1	30	36·0329	20·011
f_2	40	141·7237	46·15
$3f_1$	90	0·5721	0
$2f_1 + f_2$	100	3·5083	0
$f_1 + 2f_2$	110	7·6865	0
$3f_2$	120	5·9903	0

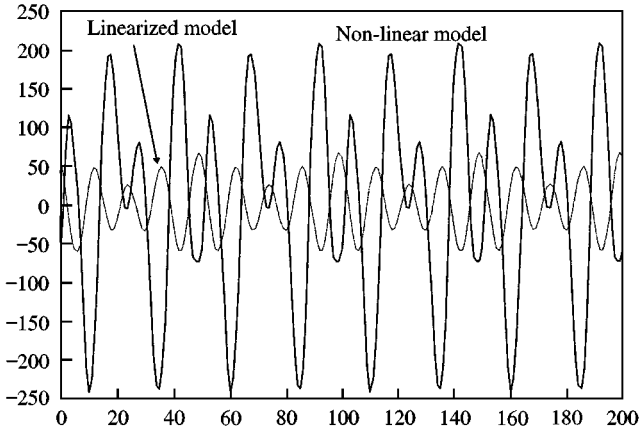

Figure 12. Intermodulation effect (——, non-linear model; – – – –, linearized model).

Note that with respect to the linearized model, not only are there significant components at new frequencies (different from either 30 or 40 Hz), such as the peak at 20 Hz, but also the components at the input frequencies are more intense. The corresponding time response (at steady state) is shown in Figure 12, where the difference in the responses of the linearized and the non-linear systems is marked.

7. CONCLUSIONS

A model identification study has been carried out on experimental data gathered at ISMES laboratories [17, 18]. The data concern a scale model of a dam buttress subjected to seismic-like excitations on a shake table. The buttress has an artificial crack and, therefore, displays a more or less non-linear behaviour, depending on the intensity of the input.

Both linear models and a suitable sub-class of the polynomial NARX/NARMAX family have been employed in the analysis. Several questions related to the identification methodology have emerged during the modelling phase; in particular, the inadequacy of classical empirical indices in the selection of the appropriate model structure is manifest. Quite satisfactory non-linear models are obtained with much fewer parameters than

suggested by these indices. Also there is no *a priori* technique to ensure that the identified model will be stable in simulation.

A second-level analysis has been performed by repeating the model identification on smaller portions of the data, to examine how the dynamic characteristics of the model can vary in time as the seismic-like excitation evolves. In this light, the authors believe that an effective structure-monitoring system should not only re-adapt the model parameters when fresh data are available, but also periodically check the validity of the model structure. Note that the last requirement prevents a straightforward implementation of classic adaptive identification algorithms.

REFERENCES

1. I. J. Leontaritis and S. A. Billings 1985 *International Journal of Control* **41**, 303–328. Input–output parametric models for non-linear systems—part I: deterministic non-linear systems.
2. I. J. Leontaritis and S. A. Billings 1985 *International Journal of Control* **41**, 329–344. Input–output parametric models for non-linear systems—part II: stochastic non-linear systems.
3. L. Ljung 1987 *System Identification: Theory For the User*. Englewood Cliffs, NJ: Prentice-Hall.
4. T. Södesrtröm and P. Stoica 1989 *System Identification*. Englewood Cliffs, NJ: Prentice-Hall.
5. E. Safak 1989 *ASCE—Journal of Engineering Mechanics* **115**, 2386–2405. Adaptive modelling, identification and control of dynamic structural systems. I: theory.
6. E. Safak 1989 *ASCE—Journal of Engineering Mechanics* **115**, 2406–2426. Adaptive modelling, identification and control of dynamic structural systems. II: applications.
7. R. K. Goel and A. K. Chopra 1997 *Report No. UCB/EERC*-97/14, *Earthquake Engineering Research Center*, *University of California at Berkeley*. Vibration properties of buildings determined from recorded earthquake motions.
8. C. H. Loh and H. M. Lin 1996 *Earthquake Engineering and Structural Dynamics* **25**, 269–290. Application of off-line and on-line identification techniques to buildings seismic response data.
9. C. H. Loh and J. Y. Duh 1996 *JSCE—Structural Engineering/Earthquake Engineering* **13**, 11–21. Analysis of nonlinear system using NARMA models.
10. P. Palumbo and L. Piroddi 2000 *Mechanical Systems and Signal Processing* **14**, 243–265. Harmonic analysis of non-linear structures by means of Generalized Frequency Response Functions coupled with NARX models.
11. M. Korenberg, S. A. Billings, Y. P. Liu and P. J. McIlroy 1987 *International Journal of Control* **48**, 193–210. Orthogonal parameter estimation algorithm for non-linear stochastic systems.
12. I. J. Leontaritis and S. A. Billings 1987 *International Journal of Control* **45**, 311–341. Model selection and validation methods for non-linear systems.
13. L. A. Aguirre and S. A. Billings 1995 *International Journal of Control* **62**, 569–587. Improved structure selection for nonlinear models based on terms clustering.
14. K. Z. Mao and S. A. Billings 1997 *International Journal of Control* **68**, 311–330. Algorithms for minimal model structure detection in nonlinear dynamic system identification.
15. S. A. Billings and K. M. Tsang 1989 *Mechanical Systems and Signal Processing* **3**, 319–359. Spectral analysis for non-linear systems, Part I: parametric non-linear spectral analysis—Part II: interpretation of non-linear frequency response functions.
16. S. A. Billings, K. M. Tsang and G. R. Tomlinson 1990 *Mechanical Systems and Signal Processing* **4**, 3–21. Spectral analysis for non-linear systems, Part III: case study examples.
17. Isмes 1996 *Prog. STR*-9019, *Doc. RAT-STR*-2485/96. Studio sperimentale su modello fisico per la valutazione di metodologie di identificazione strutturale (in Italian).
18. Isмes 1996 *Prog. STR*-9016, *Doc. RAT-STR*-2894/96. Monitoroggio dinamico delle dighe. Elaborazione in linea delle registrazioni e identificazione dei parametri strutturali (in Italian).
19. J. C. Peyton Jones and S. A. Billings 1989 *International Journal of Control* **50**, 1925–1940. Recursive algorithm for computing the frequency response of a class of non-linear difference equation model.
20. E. Safak 1988 *Open-File Report* 88-647, *U.S. Geological Survey*, *Menlo Park*, *CA*. Analysis of recordings in structural engineering: adaptive filtering, prediction and control.